

Cross-checking OSL ages from different grain sizes to improve chronological reliability in deltaic environments: an example from the Yangtze River Delta

Xuemei Wang, Xiaomei Nian*, Weiguo Zhang, Fengyue Qiu

State Key Laboratory of Estuarine and Coastal Research, East China Normal University, Shanghai

200241, China

**Corresponding author: xmlian@sklec.ecnu.edu.cn*

Table S1 Radionuclide concentrations and environmental dose rates of OSL samples from core MQ

Sample No.	Depth (m)	U (ppm)	Th (ppm)	K (%)	^a Dose rate (Gy/ka)			
					4–11 µm	45–63 µm	63–90 µm	90–125 µm
MQ-1	11.24	2.52 ± 0.10	14.00 ± 0.38	2.33 ± 0.07	3.50 ± 0.26	3.18 ± 0.21	—	—
MQ-2	21.24	1.55 ± 0.07	7.23 ± 0.23	1.93 ± 0.06	2.43 ± 0.17	2.24 ± 0.15	2.12 ± 0.14	2.10 ± 0.14
MQ-3	26.24	1.64 ± 0.08	9.37 ± 0.27	1.56 ± 0.05	2.31 ± 0.17	2.10 ± 0.14	1.97 ± 0.13	1.95 ± 0.13
MQ-4	34.23	1.39 ± 0.07	8.44 ± 0.25	1.74 ± 0.06	—	2.12 ± 0.14	2.00 ± 0.14	1.98 ± 0.13
MQ-5	47.24	1.62 ± 0.07	8.22 ± 0.25	1.81 ± 0.06	2.40 ± 0.18	2.20 ± 0.15	2.08 ± 0.14	2.06 ± 0.14
MQ-6	55.24	1.74 ± 0.08	11.70 ± 0.33	1.80 ± 0.06	—	2.43 ± 0.16	2.27 ± 0.15	2.25 ± 0.15
MQ-7	61.24	1.03 ± 0.05	5.21 ± 0.28	1.86 ± 0.06	—	—	—	1.84 ± 0.13

^aThe dose rate was calculated using DRAC (version 1.2) (Durcan et al., 2015).

Table S2 Water content results for samples collected from 15 Holocene cores in the Yangtze River Delta.

Core ID	Sample No.	Longitude (E)	Latitude (N)	Elevation (m)	Depth (m)	Water content (%)	Data source
TZK1		120°11'	32°04'	4	32.2-32.4	28.69	Cheng et al., 2021
TZK2		120°05'	32°19'	4	36.75-36.95	27.99	Cheng et al., 2021
TZ	TZ-1	119°54.845'	32°23.8317'	4.72	5.28-5.40	30 ± 5	Nian et al., 2018a
	TZ-2				21.58-21.70	31 ± 5	
	TZ-3				32.08-32.20	34 ± 5	
	TZ-4				39.08-39.20	34 ± 5	
	TZ-5				42.08-42.20	29 ± 5	
	TZ-6				51.08-51.20	31 ± 5	
	TZ-7				58.78-58.90	33 ± 5	
NT	NT-1	120°51.4'	32°3.9417'	3.99	3.78-3.90	31 ± 5	Nian et al., 2018a
	NT-2				8.78-8.90	31 ± 5	
	NT-3				12.78-12.90	33 ± 5	
	NT-4				17.78-17.90	35 ± 5	
	NT-5				27.78-27.90	34 ± 5	
	NT-6				33.78-33.90	39 ± 5	
	NT-7				36.78-36.90	33 ± 5	
	NT-8				55.78-55.90	33 ± 5	
	NT-9				59.78-59.90	34 ± 5	
SD	L58	120°46.75'	32°20.3'	4.87	8.15-8.30	27 ± 5	Nian et al., 2018b
	L5				11.15-11.30	33 ± 5	

	L59				19.15-19.30	33 ± 5	
	L6				23.15-23.30	35 ± 5	
	L60				34.15-34.30	34 ± 5	
	L61				44.65-44.80	33 ± 5	
	L62				49.65-49.80	36 ± 5	
HM	HM1	121°5'34"	31°57'25"	3.36	9.05-9.20	31 ± 10	Nian et al., 2021
	HM2				10.65-10.80	38 ± 10	
	HM3				16.65-16.80	24 ± 10	
	HM4				19.65-19.80	41 ± 10	
	HM5				23.65-23.80	27 ± 10	
	HM6				30.65-30.80	29 ± 10	
	HM7				42.65-42.80	33 ± 10	
	HM8				50.65-50.80	31 ± 10	
	HM9				61.65-61.80	33 ± 10	
CM01	L505	121°22'58.5"	31°38'28.6"		17.79	25 ± 10	Chen et al., 2021
	L514				25.85	33 ± 10	
	L542				54.05	25 ± 10	
CM02	L572	121°48'56.1"	31°32'30.5"		17.70	43 ± 10	Chen et al., 2021
	L590				35.70	31 ± 10	
	L611				56.57	26 ± 10	
HSD	L437	121°50'50"	31°18'9"		15.35	37 ± 10	Chen et al., 2021
	L458				33.95	36 ± 10	
YZ07	NL-582	121°35'49.2"	32°5'2.4"	5	0.53	22.3 ± 10	Gao et al., 2017
	NL-588				6.39	20.3 ± 10	

NL-589	6.96	20.5 ± 10
NL-590	7.84	22.9 ± 10
NL-591	9.10	24.6 ± 10
NL-592	10.06	21.4 ± 10
NL-593	11.66	29.0 ± 10
NL-594	12.16	23.7 ± 10
NL-595	13.11	26.1 ± 10
NL-596	13.60	30.5 ± 10
NL-597	14.66	20.7 ± 10
NL-599	18.41	19.7 ± 10
NL-602	20.55	26.0 ± 10
NL-603	22.09	21.2 ± 10
NL-604	23.33	20.7 ± 10
NL-606	25.00	19.4 ± 10
NL-607	26.08	18.8 ± 10
NL-608	26.16	20.0 ± 10
NL-609	28.58	18.8 ± 10
NL-610	28.95	14.7 ± 10
NL-611	29.59	19.9 ± 10
NL-612	30.30	25.1 ± 10
NL-614	32.15	22.3 ± 10
NL-616	34.48	18.0 ± 10
NL-618	36.56	17.4 ± 10
NL-619	37.48	20.7 ± 10

	NL-620		38.46	21.1 ± 10	
	NL-622		41.27	23.3 ± 10	
	NL-626		44.35	20.8 ± 10	
	NL-628		46.45	18.3 ± 10	
BX	BX-1	$121^{\circ}30'11''$	31°49'43"	2.27	37 ± 5
	BX-2			5.38	27 ± 5
	BX-3			8.35	30 ± 5
	BX-4			11.3	25 ± 5
	BX-5			14.25	30 ± 5
	BX-6			17.76	29 ± 5
	BX-7			20.87	37 ± 5
	BX-8			23.88	36 ± 5
MQ	MQ-1	$121^{\circ}30'59''$	31°54'14"	2.5	40 ± 5
	MQ-2			7	31 ± 5
	MQ-3			11.5	26 ± 5
	MQ-4			16	39 ± 5
	MQ-5			19.6	33 ± 5
	MQ-6			21.4	30 ± 5
	MQ-7			23.2	35 ± 5
	MQ-8			25.9	34 ± 5
WB	WB-1	$121^{\circ}33'2.5''$	31°57'35.7"	2.8	43 ± 5
	WB-2			7.4	37 ± 5
	WB-3			10.7	34 ± 5
	WB-4			13.3	32 ± 5

Wang et al., 2019

	WB-5			16.8	37 ± 5	
	WB-6			17.6	37 ± 5	
	WB-7			20.2	34 ± 5	
	WB-8			22.9	39 ± 5	
DY		120°37.8833'	32°24.05'	3.7	5.15–5.3 19.15–19.3	32 ± 5 34 ± 5
HA		120°19.68'	32°24.935'	4.77	5.15–5.3 19.15–19.3	33 ± 5 35 ± 5
EGQD14	NL-1051	121°41'14"	31°49'28.4"		0.9	27.0 ± 10
	NL-1055				5.0	25.1 ± 10
	NL-1058				8.3	27.3 ± 10
	NL-1060				10.1	36.0 ± 10
	NL-1063				13.0	25.5 ± 10
	NL-1066				16.1	26.5 ± 10
	NL-1071				21.0	40.6 ± 10
	NL-1073				23.1	35.1 ± 10
	NL-1077				27.1	29.3 ± 10
	NL-1080				30.0	41.3 ± 10
	NL-1083				33.1	19.6 ± 10
	NL-1086				36.0	31.4 ± 10

Table S3 Measurement protocol used for single-grain OSL sensitivity (Nian et al., 2021).

Step	Treatment	Observed
1	Blue light bleaching for 100 s at 20 °C	
2	Given dose, 20 Gy	
3	Preheat (260 °C for 10 s)	
4	Green laser stimulate for 1 s at 125 °C	L ₁
5	Test dose, 2 Gy	
6	Cut heat (220 °C for 0 s)	
7	Green laser stimulate for 1 s at 125 °C	T ₁
8	Given dose, 20 Gy	
9	Preheat (260 °C for 10 s)	
10	IR stimulation for 40 s at 20 °C	
11	Green laser stimulate for 1 s at 125 °C	L ₂
12	Test dose, 2 Gy	
13	Cut heat (220 °C for 0 s)	
14	Green laser stimulate for 1 s at 125 °C	T ₂

Note: The OSL signal intensity (L₁) was calculated as the first 0.085 s of the signal, with the background subtracted from the final 0.17 s. The ratios of L₁/T₁ and L₂/T₂ were used to check the purity of single-grain quartz. For each grain-size fraction in each sample, 15 aliquots (equivalent to 1,500 individual quartz grains) were measured.

Table S4 OSL age data for the referenced published cores from the Yangtze River Delta, as shown in Figure 1.

Core ID	Depth (m)	Grain size (μm)	U (ppm)	Th (ppm)	K (ppm)	Water content (%)	Dose rate (Gy/ka)	D_e (Gy)	Age (ka)
TZ	5.28–5.4	45–63	1.43 \pm 0.07	9.42 \pm 0.27	1.67 \pm 0.06	30 \pm 5	2.20 \pm 0.08	7.03 \pm 0.16	3.20 \pm 0.14
	21.58–21.7	45–63	1.43 \pm 0.07	10.5 \pm 0.29	1.47 \pm 0.05	31 \pm 5	2.02 \pm 0.08	7.77 \pm 0.51	3.85 \pm 0.30
	32.08–32.2	45–63	1.08 \pm 0.06	6.69 \pm 0.23	1.79 \pm 0.06	34 \pm 5	1.89 \pm 0.07	8.39 \pm 0.72	4.43 \pm 0.42
	39.08–39.2	90–125	0.63 \pm 0.04	3.99 \pm 0.15	2.06 \pm 0.06	34 \pm 5	1.76 \pm 0.07	14.01 \pm 0.95	7.95 \pm 0.62
	42.08–42.2	45–63	1.49 \pm 0.07	8.74 \pm 0.26	1.75 \pm 0.06	29 \pm 5	2.15 \pm 0.09	18.24 \pm 0.24	8.48 \pm 0.35
	51.08–51.2	45–63	1.60 \pm 0.07	9.38 \pm 0.27	1.73 \pm 0.06	31 \pm 5	2.16 \pm 0.09	17.90 \pm 0.79	8.30 \pm 0.49
	58.78–58.9	45–63	1.94 \pm 0.08	11.4 \pm 0.32	1.76 \pm 0.06	33 \pm 5	2.23 \pm 0.09	18.46 \pm 0.31	8.29 \pm 0.35
NT	3.78–3.9	45–63	3.01 \pm 0.11	11.6 \pm 0.32	1.64 \pm 0.05	31 \pm 5	2.63 \pm 0.01	2.80 \pm 0.05	1.07 \pm 0.05
	8.78–8.9	45–63	1.51 \pm 0.07	8.94 \pm 0.27	1.77 \pm 0.06	31 \pm 5	2.21 \pm 0.08	2.51 \pm 0.05	1.14 \pm 0.05
	12.78–12.9	45–63	1.28 \pm 0.06	8.88 \pm 0.27	1.63 \pm 0.05	33 \pm 5	2.00 \pm 0.08	2.55 \pm 0.06	1.28 \pm 0.06
	17.78–17.9	45–63	1.42 \pm 0.07	6.90 \pm 0.22	1.84 \pm 0.06	35 \pm 5	2.01 \pm 0.08	2.82 \pm 0.10	1.40 \pm 0.07
	27.78–27.9	45–63	1.31 \pm 0.07	7.85 \pm 0.24	1.81 \pm 0.06	34 \pm 5	2.02 \pm 0.08	15.03 \pm 0.36	7.42 \pm 0.33
	33.78–33.9	45–63	1.79 \pm 0.08	11.6 \pm 0.32	1.67 \pm 0.06	39 \pm 5	2.14 \pm 0.08	17.05 \pm 0.80	7.97 \pm 0.48
	36.78–36.9	45–63	1.22 \pm 0.06	7.72 \pm 0.25	1.74 \pm 0.06	33 \pm 5	1.96 \pm 0.08	17.67 \pm 0.39	9.02 \pm 0.40
	55.78–55.9	90–125	1.25 \pm 0.06	6.96 \pm 0.23	1.65 \pm 0.05	33 \pm 5	1.73 \pm 0.07	21.62 \pm 2.02	12.47 \pm 1.26

	59.78–59.9	90–125	2.27 ± 0.09	10.7 ± 0.3	1.62 ± 0.05	34 ± 5	2.05 ± 0.07	23.79 ± 1.83	11.58 ± 0.98
HM	9.05–9.20		1.99 ± 0.09	11.80 ± 0.33	1.62 ± 0.05	31 ± 10			0.44 ± 0.03
	10.65–10.80		1.43 ± 0.07	9.64 ± 0.28	1.83 ± 0.06	38 ± 10			0.45 ± 0.06
	16.65–16.80		1.94 ± 0.08	12.90 ± 0.36	1.72 ± 0.06	24 ± 10			0.51 ± 0.12
	19.65–19.80		2.01 ± 0.08	11.90 ± 0.33	1.87 ± 0.06	41 ± 10			2.08 ± 0.19
	23.65–23.80		1.87 ± 0.08	12.20 ± 0.34	1.79 ± 0.06	27 ± 10			2.94 ± 0.42
	30.65–30.80		1.74 ± 0.08	10.30 ± 0.29	1.85 ± 0.06	29 ± 10			3.86 ± 0.28
	42.65–42.80		1.75 ± 0.08	10.60 ± 0.30	1.74 ± 0.06	33 ± 10			7.83 ± 0.91
	50.65–50.80		1.99 ± 0.09	11.80 ± 0.33	1.85 ± 0.06	31 ± 10			6.93 ± 0.76
	61.65–61.80		1.68 ± 0.08	8.51 ± 0.26	1.65 ± 0.05	33 ± 10			9.18 ± 0.39
CM01	1.00		2.15 ± 0.02	11.80 ± 0.14	1.83 ± 0.03	25 ± 10	2.86 ± 0.18	0.31 ± 0.03	0.11 ± 0.01
	2.05		2.35 ± 0.04	12.68 ± 0.27	2.00 ± 0.01	35 ± 10	2.83 ± 0.17	0.36 ± 0.01	0.13 ± 0.01
	3.75		1.94 ± 0.04	10.84 ± 0.21	1.38 ± 0.01	26 ± 10	2.32 ± 0.15	1.42 ± 0.07	0.61 ± 0.05
	5.85		1.49 ± 0.00	8.08 ± 0.07	1.66 ± 0.01	24 ± 10	2.30 ± 0.15	1.33 ± 0.03	0.58 ± 0.04
	7.78		1.30 ± 0.01	7.45 ± 0.10	1.36 ± 0.01	20 ± 10	2.03 ± 0.14	1.24 ± 0.11	0.61 ± 0.07
	9.83		1.66 ± 0.08	9.95 ± 0.50	1.68 ± 0.08	20 ± 10	2.50 ± 0.18	1.51 ± 0.06	0.61 ± 0.05
	11.05		1.66 ± 0.02	9.11 ± 0.15	1.59 ± 0.01	20 ± 10	2.39 ± 0.17	1.43 ± 0.09	0.60 ± 0.06
	12.75		1.61 ± 0.03	8.90 ± 0.15	1.58 ± 0.02	27 ± 10	2.19 ± 0.14	1.23 ± 0.07	0.56 ± 0.05

	14.9	1.78 ± 0.02	9.46 ± 0.20	1.53 ± 0.00	22 ± 10	2.32 ± 0.16	1.33 ± 0.05	0.57 ± 0.05
	16.72	1.43 ± 0.01	7.57 ± 0.07	1.55 ± 0.01	27 ± 10	2.04 ± 0.13	1.28 ± 0.04	0.63 ± 0.05
	17.79	1.62 ± 0.02	8.41 ± 0.12	1.62 ± 0.02	25 ± 10	2.21 ± 0.15	4.78 ± 0.24	2.16 ± 0.18
	18.63	2.00 ± 0.02	10.31 ± 0.04	1.56 ± 0.02	25 ± 10	2.37 ± 0.16	5.04 ± 0.14	2.13 ± 0.15
	19.95	2.24 ± 0.04	13.18 ± 0.15	2.23 ± 0.01	42 ± 10	2.72 ± 0.16	9.52 ± 0.48	3.50 ± 0.27
	25.85	2.01 ± 0.03	10.92 ± 0.20	1.90 ± 0.01	33 ± 10	2.51 ± 0.16	16.18 ± 1.07	6.39 ± 0.59
	40.05	2.28 ± 0.06	12.24 ± 0.29	2.13 ± 0.02	27 ± 10	2.95 ± 0.20	29.87 ± 0.75	10.13 ± 0.72
	54.05	2.10 ± 0.01	11.19 ± 0.11	1.93 ± 0.01	25 ± 10	2.73 ± 0.19	31.12 ± 0.63	11.32 ± 0.81
CM02	0.25	2.04 ± 0.01	10.84 ± 0.08	1.73 ± 0.02	23 ± 10	2.79 ± 0.18	0.14 ± 0.02	0.05 ± 0.01
	0.71	1.89 ± 0.24	10.02 ± 0.04	1.72 ± 0.01	30 ± 10	2.51 ± 0.16	0.30 ± 0.03	0.12 ± 0.01
	2.98	1.73 ± 0.01	10.79 ± 0.11	1.55 ± 0.01	26 ± 10	2.41 ± 0.15	0.54 ± 0.16	0.22 ± 0.07
	5.58	1.92 ± 0.02	9.81 ± 0.16	1.57 ± 0.01	25 ± 10	2.39 ± 0.16	0.62 ± 0.05	0.26 ± 0.03
	7.43	1.83 ± 0.01	9.70 ± 0.02	1.52 ± 0.01	20 ± 10	2.43 ± 0.17	0.66 ± 0.02	0.27 ± 0.02
	10.70	1.67 ± 0.00	9.54 ± 0.08	1.83 ± 0.00	40 ± 10	2.19 ± 0.13	1.13 ± 0.08	0.52 ± 0.05
	12.91	1.44 ± 0.03	8.43 ± 0.09	1.69 ± 0.01	20 ± 10	2.37 ± 0.17	1.23 ± 0.04	0.52 ± 0.04
	14.79	1.40 ± 0.01	7.03 ± 0.04	1.71 ± 0.01	29 ± 10	2.08 ± 0.14	1.27 ± 0.04	0.61 ± 0.04
	15.67	1.38 ± 0.01	7.89 ± 0.03	1.35 ± 0.01	33 ± 10	1.79 ± 0.11	1.33 ± 0.04	0.74 ± 0.05
	16.95	2.17 ± 0.11	14.30 ± 0.72	2.38 ± 0.12	46 ± 10	2.78 ± 0.17	4.04 ± 0.24	1.45 ± 0.13

	17.70	1.96 ± 0.01	12.32 ± 0.27	2.41 ± 0.03	43 ± 10	2.72 ± 0.16	4.38 ± 0.08	1.61 ± 0.10
	19.70	1.99 ± 0.10	11.90 ± 0.60	1.85 ± 0.09	38 ± 10	2.41 ± 0.16	6.70 ± 0.30	2.78 ± 0.22
	20.70	1.91 ± 0.02	10.70 ± 0.11	1.62 ± 0.01	32 ± 10	2.28 ± 0.14	6.74 ± 0.13	2.96 ± 0.20
	24.65	2.00 ± 0.06	11.87 ± 0.45	2.23 ± 0.02	39 ± 10	2.66 ± 0.16	7.81 ± 0.34	2.93 ± 0.22
	30.70	2.07 ± 0.02	12.58 ± 0.23	2.40 ± 0.02	43 ± 10	2.74 ± 0.16	9.74 ± 0.53	3.56 ± 0.29
	32.70	1.95 ± 0.01	11.34 ± 0.10	2.12 ± 0.01	35 ± 10	2.63 ± 0.16	10.66 ± 0.22	4.06 ± 0.27
	33.70	2.08 ± 0.03	11.87 ± 0.21	2.25 ± 0.01	37 ± 10	2.72 ± 0.17	11.67 ± 0.25	4.29 ± 0.28
	35.70	2.00 ± 0.02	10.70 ± 0.10	2.00 ± 0.01	31 ± 10	2.59 ± 0.17	23.20 ± 0.53	8.97 ± 0.61
	39.70	1.95 ± 0.03	12.15 ± 0.18	2.09 ± 0.01	31 ± 10	2.75 ± 0.18	29.71 ± 0.82	10.81 ± 0.76
	45.70	1.90 ± 0.03	10.32 ± 0.13	1.80 ± 0.01	34 ± 10	2.33 ± 0.15	25.73 ± 1.27	11.05 ± 0.88
HSD	0.84	2.35 ± 0.04	11.78 ± 0.24	1.94 ± 0.02	38 ± 10	2.69 ± 0.16	0.35 ± 0.02	0.13 ± 0.01
	1.73	1.76 ± 0.02	9.25 ± 0.10	1.75 ± 0.00	41 ± 10	2.23 ± 0.12	0.40 ± 0.01	0.18 ± 0.01
	3.89	1.66 ± 0.01	8.64 ± 0.04	1.66 ± 0.01	37 ± 10	2.15 ± 0.13	0.39 ± 0.03	0.18 ± 0.02
	5.78	1.66 ± 0.02	8.90 ± 0.11	1.50 ± 0.01	32 ± 10	2.10 ± 0.13	0.55 ± 0.03	0.26 ± 0.02
	7.55	1.02 ± 0.00	6.28 ± 0.07	1.74 ± 0.02	32 ± 10	1.99 ± 0.13	0.51 ± 0.04	0.26 ± 0.03
	9.45	2.21 ± 0.03	11.41 ± 0.15	1.88 ± 0.01	35 ± 10	2.55 ± 0.15	0.68 ± 0.06	0.27 ± 0.03
	10.85	1.80 ± 0.09	9.98 ± 0.50	1.72 ± 0.09	34 ± 10	2.27 ± 0.15	0.83 ± 0.10	0.37 ± 0.05
	11.45	1.79 ± 0.03	10.18 ± 0.10	1.70 ± 0.01	38 ± 10	2.20 ± 0.13	0.80 ± 0.04	0.36 ± 0.03

13.25		1.65 ± 0.04	9.73 ± 0.02	1.61 ± 0.01	36 ± 10	2.11 ± 0.13	0.85 ± 0.02
14.2		1.69 ± 0.02	9.78 ± 0.19	1.57 ± 0.01	35 ± 10	2.11 ± 0.13	0.79 ± 0.08
15.35		1.87 ± 0.01	11.15 ± 0.09	1.81 ± 0.01	37 ± 10	2.37 ± 0.14	3.56 ± 0.20
16.95		2.10 ± 0.00	12.64 ± 0.11	2.21 ± 0.02	48 ± 10	2.55 ± 0.14	4.32 ± 0.13
20.55		2.12 ± 0.03	13.14 ± 0.20	2.34 ± 0.02	50 ± 10	2.61 ± 0.15	7.31 ± 0.44
22.25		2.05 ± 0.02	12.41 ± 0.11	2.17 ± 0.02	48 ± 10	2.49 ± 0.14	9.38 ± 0.39
33.95		2.42 ± 0.12	13.40 ± 0.67	2.14 ± 0.11	36 ± 10	2.81 ± 0.19	21.78 ± 0.95
34.85		1.94 ± 0.04	10.33 ± 0.21	1.75 ± 0.01	31 ± 10	2.37 ± 0.15	24.93 ± 0.60
							10.51 ± 0.72

Table S5 AMS ^{14}C ages of cores JD01 and HQ98 from the Yangtze River Delta. All ages have been converted to ka (relative to 2013 AD) for consistency with OSL ages.

Core ID	Depth (m)	elevation (m)	Dating material	$\delta^{13}\text{C}$ (‰)	Conventional age		Calibrated age (cal. yr BP)			ka (relative to 2013AD)	Lab number
					a BP	err	2 sigma	Prob.	Median		
JD01	-7.07	-1.37	Mollusk shell	-9.7	5590	50	5593–5937	1	5765	5.83	Beta-254176
	-12.09	-6.39	Plant fragments	-28	6570	50	7421–7571	0.98	7496	7.56	Beta-254177
	-14.14	-8.44	Mollusk shell	-8.4	5570	50	5585–5919	1	5752	5.82	Beta-254178
	-16.42	-10.72	Mollusk shell	-9.9	5170	40	5148–5515	1	5332	5.39	Beta-254179
	-22.38	-16.68	Mollusk shell	-9.6	5270	40	5291–5585	1	5438	5.50	Beta-254180
	-23.82	-18.12	Mollusk shell	-9.8	5430	40	5445–5781	1	5613	5.68	Beta-254181
	-24.38	-18.68	Mollusk shell	-10.4	5580	40	5598–5916	1	5757	5.82	Beta-254182
	-25.99	-20.29	Plant fragments	-28.5	5280	40	5936–6188	1	6062	6.13	Beta-254183
	-27.21	-21.51	Plant fragments	-27.4	5910	40	6645–6800	0.94	6723	6.79	Beta-254184
	-28.2	-22.5	Plant fragments	-28.5	5260	40	5929–6182	1	6056	6.12	Beta-254185
	-29	-23.3	Mollusk shell	-9.3	5710	40	5735–6102	1	5919	5.98	Beta-254186
	-30.05	-24.35	Mollusk shell	-9.4	5500	40	5538–5871	1	5705	5.77	Beta-254187
	-31.07	-25.37	Mollusk shell	-9.9	5720	40	5742–6110	1	5926	5.99	Beta-254188
	-31.79	-26.09	Plant fragments	-27.4	6080	40	6795–7023	0.91	6909	6.97	Beta-254189

-32.85	-27.15	Plant fragments	-27.6	5730	40	6437–6636	0.96	6537	6.60	Beta-254190	
-33.82	-28.12	Plant fragments	-27.3	5780	40	6483–6672	0.99	6578	6.64	Beta-254191	
-40.15	-34.45	Mollusk shell	-10.9	5970	40	6008–6346	1	6177	6.24	Beta-254192	
-41.94	-36.24	Mollusk shell	-9.9	5700	40	5726–6093	1	5910	5.97	Beta-254193	
-44.9	-39.2	Mollusk shell	-12.1	6080	40	6162–6476	1	6319	6.38	Beta-254194	
HQ98	0.7	5.21	snail shell	-4.6	520	50	494–643	1	568.5	0.63	Beta-130653
	4.7	1.21	Mollusk shell	-7.6	4410	50	4158–4569	1	4363.5	4.43	Beta-130654
	5.5	0.41	Mollusk shell	-9	5490	30	5533–5854	1	5693.5	5.76	Beta-132941
	6.15	-0.24	Mollusk shell	-7.1	5870	60	5908–6269	1	6088.5	6.15	Beta-130655
	13.3	-7.39	Mollusk shell	-9.1	4570	50	4403–4796	1	4599.5	4.66	Beta-130656
	23.2	-17.29	Mollusk shell	-6.4	5620	60	5605–5991	1	5798	5.86	Beta-130657
	28.6	-22.69	Mollusk shell	-4.6	7170	70	7290–7640	1	7465	7.53	Beta-130658
	30.12	-24.21	Plant	-28.4	8080	70	8719–9143	0.92	8931	8.99	Beta-130659
	42.75	-36.84	Plant	-26.9	9050	120	9268–9967	1	9617.5	9.68	Beta-130660
	48.32	-42.41	Mollusk shell	-10.3	10490	80	11246–11835	1	11540.5	11.60	Beta-130661
52.65	-46.74	Mollusk shell	-9.3	10710	70	11606–12235	1	11920.5	11.98	Beta-130662	
53.8	-47.89	Mollusk shell	-7.8	10780	90	11695–12399	1	12047	12.11	Beta-130663	
55.5	-49.59	Mollusk shell	-9.2	10510	70	11282–11850	1	11566	11.63	Beta-130664	

57	-51.09	Mollusk shell	-8.4	10420	70	11204–11722	1	11463	11.53	Beta-130665
57.95	-52.04	Mollusk shell	-10.2	10480	40	11296–11758	1	11527	11.59	Beta-132942

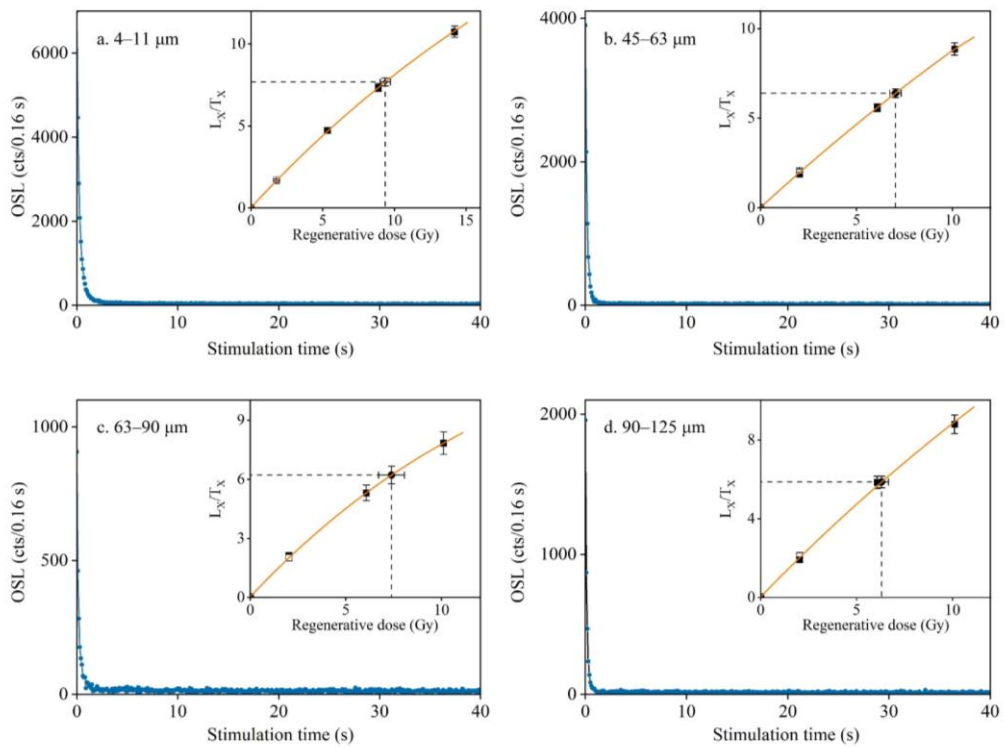


Figure S1. Natural decay curves alongside the corresponding growth curves for different quartz grain-size fractions of sample MQ-3.

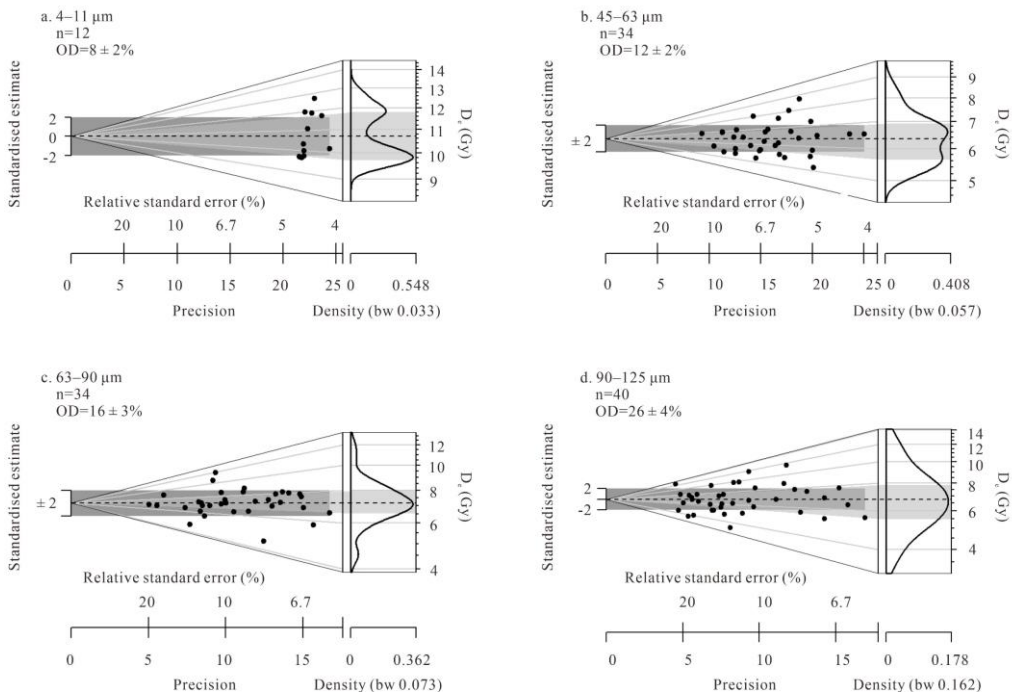


Figure S2. Abanico plots showing the D_e distributions for different quartz grain-size fractions of sample MQ-3.

References

- Chen, Y. L., Zhang, W. G., Nian, X. M., Sun, Q. L., Ge, C., Hutchinson, S. M., et al. (2021). Greigite as an indicator for salinity and sedimentation rate change: Evidence from the Yangtze River Delta, China. *J. Geophys. Res. Solid Earth.* 126, e2020JB021085. doi: 10.1029/2020JB021085
- Cheng, Y., Zou, X. Q., Li, X. Q., Zhao, Z. Y., Zhang, X. Y., Guo, G., et al. (2021). Sedimentary characteristics and evolution process of the Huangqiao sand body in the Yangtze River Delta, China. *Estuar. Coast. Shelf Sci.* 107330. doi: 10.1016/j.ecss.2021.107330
- Gao, L., Long, H., Shen, J., Yu, G., Liao, M., Yin, Y. (2017). Optical dating of Holocene tidal deposits from the southwestern coast of the South Yellow Sea using different grainsize quartz fractions. *J. Asian Earth Sci.* 135, 155–165. doi: 10.1016/j.jseas.2016.12.036
- Gao, L., Long, H., Zhang, P., Tamura, T., Feng, W., Mei, Q. (2019). The sedimentary evolution of Yangtze River delta since MIS3: a new chronology evidence revealed by OSL dating. *Quat. Geochronol.* 49, 153–158. doi: 10.1016/j.quageo.2018.03.010
- Nian, X., Zhang, W., Wang, Z., Sun, Q., Chen, J., Chen, Z. (2018a). Optical dating of Holocene sediments from the Yangtze River (Changjiang) delta, China. *Quat. Int.* 467, 251–263. doi: 10.1016/j.quaint.2018.01.011
- Nian, X., Zhang, W., Wang, Z., Sun, Q., Chen, J., Chen, Z., et al. (2018b). The chronology of a sediment core from incised valley of the Yangtze River delta: comparative OSL and AMS ^{14}C dating. *Mar. Geol.* 395, 320–330. doi: 10.1016/j.margeo.2017.11.008
- Nian, X., Zhang, W., Wang, Z., Sun, Q., Chen, Z. (2021). Inter-comparison of optically stimulated luminescence (OSL) ages between different fractions of Holocene deposits from the Yangtze delta and its environmental implications. *Mar. Geol.* 432, 106401. doi: 10.1016/j.margeo.2020.106401
- Wang, F., Zhang, W., Nian, X., Ge, C., Zhao, X., Cheng, Q., et al. (2019). Refining the late-Holocene coastline and delta development of the northern Yangtze River delta: Combining historical archives and OSL dating. *Holocene.* 29(9), 1439–1449. doi: 10.1177/0959683619854522
- Wang, Z., Saito, Y., Zhan, Q., Nian, X., Pan, D., Wang, L., et al. (2018). Three-dimensional evolution of the Yangtze River mouth, China during the Holocene: Impacts of sea level, climate and human activity. *Earth. Sci. Rev.* 185, 938–955. doi: 10.1016/j.earscirev.2018.08.012